AGU ADVANCING EARTH AND SPACE SCIENCE

Geophysical Research Letters®

RESEARCH LETTER
10.1029/2022GL098700

Drought Legacy in Sub-Seasonal Vegetation State and Sensitivity to Climate Over the Northern Hemisphere

Minchao Wu[1,2], Stefano Manzoni[3,4], Giulia Vico[5], Ana Bastos[6], Franciska T. de Vries[7], and Gabriele Messori[1,4,8,9]

[1]Department of Earth Sciences, Uppsala University, Uppsala, Sweden, [2]Department of Physical Geography and Ecosystem Science, Lund University, Lund, Sweden, [3]Department of Physical Geography, Stockholm University, Stockholm, Sweden, [4]Bolin Centre for Climate Research, Stockholm University, Stockholm, Sweden, [5]Department of Crop Production Ecology, Swedish University of Agricultural Sciences (SLU), Uppsala, Sweden, [6]Department of Biogeochemical Integration, Max-Planck Institute for Biogeochemistry, Jena, Germany, [7]Institute for Biodiversity and Ecosystem Dynamics, University of Amsterdam, Amsterdam, The Netherlands, [8]Centre of Natural Hazards and Disaster Science (CNDS), Uppsala University, Uppsala, Sweden, [9]Department of Meteorology, Stockholm University, Stockholm, Sweden

Key Points:

- Prominent increases in the sensitivity of herbaceous vegetation to hydrological conditions after severe droughts in the high-latitudes
- Significant vegetation greening in the 2–6 growing-season months following severe droughts
- Larger drought legacy effects on the sensitivity of herbaceous vegetation to climate compared with woody vegetation

Supporting Information:

Supporting Information may be found in the online version of this article.

Correspondence to:

M. Wu,
minchao.wu@geo.uu.se

Citation:

Wu, M., Manzoni, S., Vico, G., Bastos, A., de Vries, F. T., & Messori, G. (2022). Drought legacy in sub-seasonal vegetation state and sensitivity to climate over the Northern Hemisphere. *Geophysical Research Letters*, *49*, e2022GL098700. https://doi.org/10.1029/2022GL098700

Received 13 MAR 2022
Accepted 7 JUL 2022

Author Contributions:

Conceptualization: Minchao Wu, Stefano Manzoni, Giulia Vico, Ana Bastos, Gabriele Messori
Data curation: Minchao Wu
Formal analysis: Minchao Wu
Funding acquisition: Minchao Wu, Stefano Manzoni, Giulia Vico, Gabriele Messori
Investigation: Minchao Wu
Methodology: Minchao Wu, Stefano Manzoni, Giulia Vico, Ana Bastos, Gabriele Messori
Project Administration: Minchao Wu, Gabriele Messori
Resources: Minchao Wu
Software: Minchao Wu

Abstract Droughts affect ecosystems at multiple time scales, but their sub-seasonal legacy effects on vegetation activity remain unclear. Combining the satellite-based enhanced vegetation index MODIS EVI with a novel location-specific definition of the growing season, we quantify drought impacts on sub-seasonal vegetation activity and the subsequent recovery in the Northern Hemisphere. Drought legacy effects are quantified as changes in post-drought greenness and sensitivity to climate. We find that greenness losses under severe drought are partially compensated by a ~+5% greening within 2–6 growing-season months following the droughts, both in woody and herbaceous vegetation but at different timings. In addition, post-drought sensitivity of herbaceous vegetation to hydrological conditions increases noticeably at high latitudes compared with the local normal conditions, regardless of the choice of drought time scales. In general, the legacy effects on sensitivity are larger in herbaceous vegetation than in woody vegetation.

Plain Language Summary Droughts are increasingly severe and widespread globally, but their impacts on the global carbon cycle remain unclear due to the complexity of vegetation response to climate under and after droughts. In particular, how much plant activity decreases during drought and how quickly it recovers in the following months or years is not well understood. Here, by employing large-scale satellite-derived vegetation information, we identify the existence of widespread drought legacy effects on vegetation activity in the Northern Hemisphere ecosystems. We find that vegetation becomes greener in 2–6 growing-season months after severe droughts with a stronger response to climate. These findings are in general more prominent at mid- and high-latitudes, in particular for the grass-dominated ecosystems compared with the tree-dominated ones. Our analyses extend the picture for understanding how vegetation responds to severe droughts and could provide useful information to assist the development of dynamic vegetation models toward assessing changes in ecosystem resilience under changing climates.

1. Introduction

Droughts impact ecosystem functioning worldwide (Allen et al., 2010, 2015; Orth et al., 2020; Reichstein et al., 2013). They affect vegetation activity directly by reducing photosynthesis and transpiration (Bréda et al., 2006; Iturbe-Ormaetxe et al., 1998; Poorter et al., 2012). The impacts of droughts, especially when severe, can last beyond the dry period, and affect ecosystem functioning for days to years, depending on drought intensity and duration (Allen et al., 2015; L. D. L. Anderegg et al., 2013; Z. Xu et al., 2010), vegetation type (Scherrer et al., 2011), and plant community composition (Fauset et al., 2012). These legacy effects may be due to structural damages at the individual scale (Ruehr et al., 2019; Trugman et al., 2018), or vegetation mortality and changes in community composition (Cailleret et al., 2017). Furthermore, droughts can also alter soil processes, for example, nutrient availability, which in turn affects vegetation activity at multiple temporal scales (Gessler et al., 2017). Given the projected increase in drought risk in many regions in the Northern Hemisphere under anthropogenic warming (Diffenbaugh et al., 2015; Pastorello et al., 2020; Prudhomme et al., 2014), we expect that drought will become increasingly important for ecosystem states and impose profound impacts on the regional and global

Supervision: Stefano Manzoni, Giulia Vico, Gabriele Messori
Validation: Minchao Wu
Visualization: Minchao Wu
Writing – original draft: Minchao Wu
Writing – review & editing: Minchao Wu, Stefano Manzoni, Giulia Vico, Ana Bastos, Franciska T. de Vries, Gabriele Messori

carbon cycle (Seneviratne et al., 2012; van der Molen et al., 2011; Vicente-Serrano et al., 2020; Wu, Smith, et al., 2021; C. Xu et al., 2019).

Vegetation recovery after drought (i.e., post-drought recovery) depends on complex physiological and ecological mechanisms acting at multiple spatio-temporal scales. Post-drought recovery of leaf water potential and cell turgor can occur within hours after re-wetting, while leaf hydraulics and leaf gas exchange can take up to 1 month to recover (Blackman et al., 2009; Brodribb et al., 2010; Posch et al., 2009; Ruehr et al., 2019). The resultant decoupling of assimilation rate from transpiration is usually short-term (Gallé et al., 2007; Resco et al., 2009), and effects are longer on radial stem growth (W. R. L. Anderegg et al., 2015). If drought-related damage occurs, carbon fluxes can be decoupled from growing conditions following the event. In some cases, recovery may fail, for example, due to the limited availability of non-structural carbon reserves to repair drought-induced damage and regrow in the next growing season (Hartmann et al., 2016; Mencuccini et al., 2015). In these cases, trees are likely more vulnerable to subsequent disturbances (e.g., Steele et al., 1995) or climate extremes (e.g., Adams et al., 2009), leading to higher mortality after droughts and changes in demography (e.g., age structure) and ultimately vegetation composition (Clark et al., 2016; Reichstein et al., 2013). While the long-term (e.g., longer than a year), or small-scale (e.g., pot experiments or field measurements) legacy effects on different aspects of the carbon cycle have been extensively explored (e.g., W. R. L. Anderegg et al., 2015), legacy effects at intermediate temporal scales (e.g., within one or two growing seasons) are still poorly understood over large geographical scales. In particular, the post-drought vegetation sensitivity to climatic conditions remains largely unexplored.

The challenge of assessing large-scale sub-seasonal legacy effects lies not only in the complexity of the processes involved but also in the availability of observations at appropriate spatial and temporal scales. For example, field measurements provide comprehensive information on vegetation processes, but extreme events are intrinsically seldom observed. Remote sensing provides an increasingly extensive spatial and temporal coverage, offering a tool to tackle this challenge, particularly when assessing changes in vegetation states such as canopy cover and density (e.g., leaf area index) and vegetation water content in a large-scale context (Jiao et al., 2021; Konings et al., 2019; McDowell et al., 2015). While legacy effects in specific regions or at specific time scales (e.g., for a single extreme event or aggregation at an annual scale) have been conducted (Bastos et al., 2021b; Brun et al., 2020; Gazol et al., 2018; Kannenberg et al., 2019; X. Wu et al., 2018), a systematic analysis of sub-seasonal legacy effects for Northern Hemisphere ecosystems is lacking.

Here, we explore the post-drought changes in vegetation state and sensitivity to climate in the first two growing seasons over the Northern Hemisphere using the Moderate Resolution Imaging Spectroradiometer (MODIS) enhanced vegetation index (EVI). To understand legacy effects on vegetation activity, we isolate phenology signals within the growing season and minimize the abiotic noise (e.g., induced by bare soil and snow) from the non-growing season that may confound the interpretation of post-drought vegetation dynamics. Commonly-used estimates of vegetation recovery are based on the absolute elapsed time after drought and may include noise from dormant periods (Figure S1 in Supporting Information S1). Furthermore, calculations are often performed based on fixed calendar months, which may overlook phenological differences induced by heterogeneous land surfaces (e.g., lowlands vs. mountains) or local climatic conditions in large-scale analyses, thus confounding the interpretation of drought responses.

To resolve the heterogeneity of sub-growing-season vegetation dynamics, we adopt a novel analytical approach using a location-specific definition of the growing season (Wu, Vico, et al., 2021). We consider the possible confounding effect of climate anomalies following the drought period and standardized post-extreme vegetation response to climate. Drought legacy effects (based on EVI) are quantified as changes in vegetation states and sensitivity to post-drought climate across different ecosystems in the Northern Hemisphere. Through this analysis, we aim to understand the drought legacy effects as: (a) how vegetation recovery in the Northern Hemisphere differs across ecosystems after severe droughts and (b) how vegetation sensitivity to climatic conditions changes in the post-drought periods.

2. Data and Methods

2.1. Data

To estimate the vegetation-climate relationships under and after drought (defined as hydrological imbalance; Huschke [1959]), we analyzed changes in vegetation state using the MODIS EVI (MOD13C1 v006 with 16-day

and 0.05° resolutions), against drought severity represented by the Standardized Precipitation-Evapotranspiration Index, SPEI (Vicente-Serrano et al., 2010), at the time scales of 1 month (SPEI1), 3 months (SPEI3), and 6 months (SPEI6), and key growing conditions, including 2m air temperature, downwards surface solar radiation derived from ERA5 reanalysis at 0.25°(Hersbach et al., 2020), and root-zone soil moisture (0.25°) from the Global Land Evaporation Amsterdam Model (GLEAM, Martens et al. [2017]). Other ancillary datasets such as frost day frequency from CRU TS 4.05 at 0.5° (Harris et al., 2020), MODIS land cover data set at 0.05° (Friedl et al., 2002), Global Aridity Index at 30 arc-seconds, and ESA CCI Land Cover at 300m were also used. To ensure consistency, all datasets were harmonized to a monthly (except for the annual land cover class data set) and 0.5° spatial resolution aggregated from their original resolutions for the Northern Hemisphere (>23°N). The period common to all datasets, 2001–2020, was used unless otherwise specified. We refer readers to Supporting Information S1 for more details.

2.2. Identifying Growing Season, Drought Events, and Post-Drought Periods

We employed a location-specific definition of the growing season to infer vegetation responses after drought events (Figure S1 in Supporting Information S1), based on vegetation phenology (Wu, Vico, et al., 2021). First, the 20-year mean of grid-specific key growing season (GS) parameters were calculated (Figure S2 in Supporting Information S1): the starting month of the growing season (SOS), the month corresponding to the peak of the growing season (POS), and the ending month of the growing season (EOS). Based on these, for each grid point over different land cover classes (Figure S3 in Supporting Information S1), we determined the lengths of the whole growing season (LOS = EOS-SOS), and early growing season (EGS = POS-SOS), and late growing season (LGS = EOS-POS).

We defined the severe drought months (m_{ex}) as the GS months with SPEI less than −1.5. Post-drought months ($m_1, \ldots m_n$, with $n = 12$) start from the first month after the end of the drought (m_{ex}) and are only counted within the location-specific GS period. They thus do not include the vegetation dormant period (months before SOS and after EOS, Figure S1 in Supporting Information S1).

Severe-drought impacts were evaluated based on the standardized GS EVI anomalies. These anomalies were extracted for each gridpoint after detrending and deseasonalizing the values within the location-specific GS and were standardized as a percentage of the climatological (i.e., average over the period in analysis) peak of EVI. For growing condition data (temperature, radiation, and soil moisture), a similar approach was applied, but anomalies were standardized in z-score (i.e., normalized by the standard deviation). This allows a standardized comparison of the vegetation sensitivities to climate quantities which differ greatly in physical units.

2.3. Estimates of Post-Drought Vegetation Recovery and Post-Drought Vegetation Sensitivity to Climate Conditions

We quantified the drought legacy effects on vegetation state and sensitivity based on the standardized GS anomalies of EVI and climatic conditions. Only areas with negative drought impacts on EVI (i.e., negative GS month anomalies under severe drought) were included for analysis (Figure 1). Post-drought vegetation changes may be affected by concurrent climate variability (Bastos et al., 2021a), favorable climatic conditions could facilitate post-drought recovery, while adverse conditions could impair recovery. Here, we assessed changes in vegetation state and sensitivity of vegetation to the concurrent climate conditions, both of which serve as indicators of legacy effects from drought events. We used robust linear regression models (Dumouchel et al., 1992) based on the standardized GS anomalies for two periods: (a) normal periods (NM): all months excluding those in the years with extreme SPEI values and post-drought months, and (b) post-drought periods (PD): only months after a severe drought ($m_1, \ldots m_n$). Specifically, the GS EVI anomalies (Y) (Figures S4-S8 in Supporting Information S1) are assumed to be a linear function of climatic variables (X). The number of points in each regression corresponds to the number of gridpoints times the number of temporal points, which depends on GS length and the number of drought events. The intercept of the regression line (α) represents a theoretical vegetation state under normal climate conditions (i.e., without anomalies), while the slope (β) reflects the vegetation sensitivity to climate. This linear regression was calculated for both NM and PD conditions:

$$Y_{t,k} = \alpha_{t,i,k} + \beta_{t,i,k} \times X_{t,i,k} + error \quad (1)$$

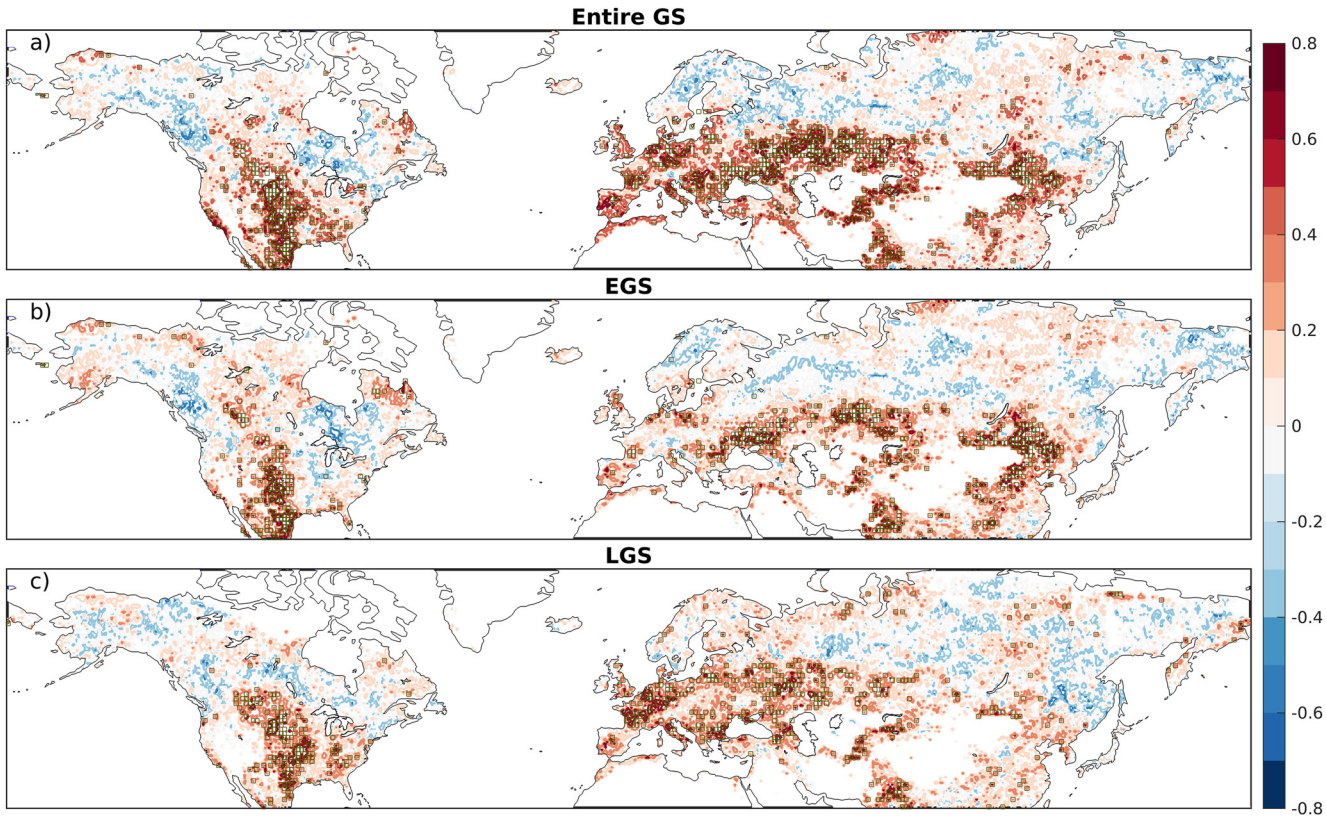

Figure 1. Water-limited regions indicated by grid-wise Pearson correlation coefficient (*r*, contour) between enhanced vegetation index (EVI) and Standardized Precipitation-Evapotranspiration Index at time scale of 1 month (SPEI1) during 2001–2020 for the Northern-Hemisphere vegetated regions. (a) *r* is calculated based on the GS-based standardized anomalies of EVI and SPEI1; (b) and (c) are the early GS (EGS) and late GS (LGS) respectively (see the definition of GS, EGS, and LGS in Section 2.2). Gray squares indicate vegetated areas which have experienced severe droughts (defined as SPEI1<−1.5) with negative impacts on vegetation states (i.e., negative EVI anomalies). These areas account for 60%, 56%, and 57% of the significantly drought-affected areas (i.e., locations with significant *r* in Figure S4 in Supporting Information S1) for the entire GS, EGS, and LGS, respectively.

where $Y_{t,k}$ represents the standardized GS EVI anomalies for period t (*i.e.*, NM or PD period) and land cover class k, and $X_{t,i,k}$ represents standardized GS anomalies of one of the climatic conditions considered (subscript i refers to SPEI, temperature, radiation or soil moisture) during period t and for land cover class k. Therefore, the legacy effect for the average vegetation state ($\alpha_{leg,i,k}$) and sensitivity ($\beta_{leg,i,k}$) to each climate condition (i) and land cover class (k) can be quantified as the differences between the corresponding parameters of the NM and PD periods, represented as:

$$\alpha_{leg,i,k} = \alpha_{PD,i,k} - \alpha_{NM,i,k} \quad (2)$$

$$\beta_{leg,i,k} = \beta_{PD,i,k} - \beta_{NM,i,k} \quad (3)$$

We analyzed the post-drought impacts on vegetation state and its sensitivity to climate focusing on drought-affected areas (i.e., gridpoints with significant SPEI-EVI correlation coefficient, verified as being least overlapped with heavily irrigated areas, Figure S4 in Supporting Information S1), with negative impacts during EGS. The analysis based on EGS was less affected by the following dormant period and better captured the legacy effects. SPEI1 was chosen to illustrate the legacy effects of the intense meteorological droughts (Zolina et al., 2013) which usually occur within 1 month. Since drought impacts may depend on drought duration, additional analyses based on SPEI3 and SPEI6 were also conducted to investigate the dependence of legacy effects on SPEI time scales. Droughts with negative impacts during LGS were also analyzed and compared with the ones for EGS droughts in Supporting Information S1. To distinguish between energy- and water-limited ecosystems, we calculated the recovery trajectory by analyzing ecosystems with different GS lengths separately (Figure 2) given the fact that GS length reflects the combined effects of both temperature and water availability. In addition, because of the

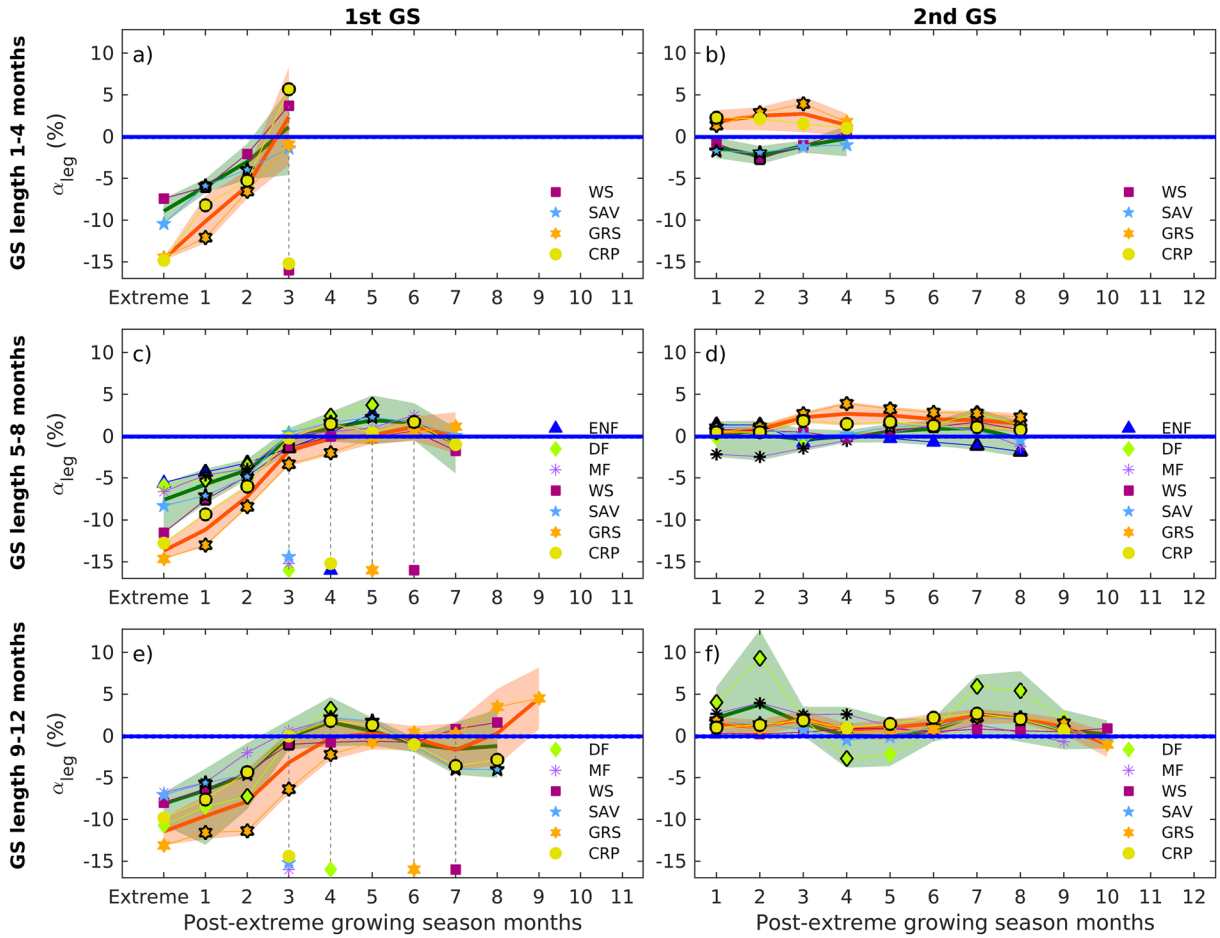

Figure 2. Recovery trajectories represented as standardized changes in land cover class-averaged vegetation state (α_{leg}) during the post-drought periods for the Northern Hemisphere when a severe drought occurs during the early GS. First GS indicates the growing season when a severe drought occurs (left column), second GS indicates the following growing season (right column); for both growing seasons, results are shown separately for short (top row), intermediate (middle row) and long (bottom row) GS length. The colors refer to land cover classes: ENF, evergreen needleleaf forests; DF, deciduous forests; MF, mixed forests; WS, closed shrubland, open shrubland, and woody savannas; SAV, savannas (temperate); GRS, grasslands; CRP, croplands. Only gridpoints with a significant correlation between EVI anomalies and SPEI1 ($p < 0.05$) and with negative drought impacts on EVI are included. The thick solid lines and the shaded area in dark green indicate the mean of all the woody vegetation, and the standard error of the mean, respectively. The dark orange ones are for herbaceous vegetation. Dots with black edges indicate that α_{leg} is significantly different ($p < 0.05$) from zero. The woody vegetation includes ENF, DF, MF, WS, and SAV wherever available, and the herbaceous vegetation includes GRS and CRP. Dashed lines indicate the month when EVI recovers back to the normal state for a specific land cover class.

spatial aggregation, we expected the detected legacy effects to cancel out, at least partly depending on the spatial heterogeneity within the aggregation group. Analyses considering aridity impacts are also provided in Supporting Information S1.

3. Results

3.1. Seasonally-Varying Hydrological Controls Over the Northern Hemisphere

The spatial pattern of grid-wise Pearson correlation coefficient (r) between EVI and SPEI1 provides an overall picture of water-limited areas over the Northern Hemisphere (Figure 1a). Highly positive and significant r between the GS-average SPEI1 and EVI occur in mid- and low-latitude regions (e.g., southern and central Europe, northern China, and large parts of North America up to around 59°N). These areas are generally not intensively irrigated (Figure S4 in Supporting Information S1). Moderately negative r between EVI and SPEI1 indicating an energy-limited regime in which vegetation benefits from drier conditions, occurs for vegetation at high latitudes such as Canada, Scandinavia, and Russia (Figure 1a). Approximately 24% of the vegetated areas in the analyzed domain have experienced severe droughts with negative impacts on vegetation states (gray squares),

which are mainly over positive-r areas. In the following, we focus on areas with negative impacts on EVI induced by severe droughts (i.e., areas with positive r values and gray squares).

The negative impacts of severe droughts are not equally distributed between the two GS sub-periods, EGS and LGS. In Europe, these impacts mainly appear during LGS, although the cases for EGS in specific regions are also found, such as northern England and Germany (Figures 1b and 1c). By contrast, in northern China, the impacts mainly appear in EGS. Inland North America and Central Asia have comparable spatial distributions of drought impacts during EGS and LGS (Figures 1b and 1c).

3.2. Vegetation Recovery Trajectories

We analyzed the post-drought changes in EVI focusing on the severe droughts that decreased EVI (Figure 1). For most ecosystems, EVI recovers within the first GS, within three to seven GS months (Figure 2). Ecosystems with LOS of 1–4 months, which generally correspond to the high-latitude vegetated regions (Figure S2d in Supporting Information S1), differ greatly in recovery. For example, closed shrubland (WS) and croplands (CRP) EVI fully recover before the end of GS, while temperate savannas (SAV) and grasslands (GRS) do not, but approach their climatological states by the end of GS (Figure 2a). The ecosystems with LOS of 5–12 months, largely located in the mid- and low-latitudes, recover within the first GS, with the longest recovery for WS (Figures 2c and 2e). Also, a certain extent of greening (up to +5%) is found for woody vegetation, generally around 2–6 growing-season months after the severe drought. Overall, herbaceous vegetation tends to be more vulnerable (a larger EVI decrease under a severe drought, up to −20%; Figure S15 in Supporting Information S1), but also more resilient (a steeper EVI recovery trajectory) than woody vegetation during the first GS.

During the second GS, the negative impacts on vegetation greenness from the previous drought (negative α_{leg}) become marginal. Instead, a positive legacy is found for herbaceous vegetation reflecting a certain degree of greening, with the most pronounced effect (∼+5%) in shorter-LOS ecosystems (Figures 2b, 2d and 2f), and especially in the arid regions (Figure S15 in Supporting Information S1).

3.3. Drought Legacy Effects Increase Sensitivity to Climate Conditions

Next, we analyzed the legacy effects on vegetation sensitivity to climate. Such effects vary between short- and long-GS length ecosystems and between woody and herbaceous vegetation (Figure 3). Specifically, during the normal periods (black signs at the bottom of each panel in Figure 3), EVI of woody vegetation with LOS of 1–8 months generally correlates negatively with SPEI1 (black '−' signs) and positively to temperature and radiation (black '+' signs; Figures 3a–3d). This indicates that woody vegetation is normally not water-, but energy-limited. Conversely, EVI in herbaceous vegetation is positively correlated with SPEI1 ('+' signs) and negatively correlated with temperature, suggesting water-limitation. Ecosystems with LOS of 9–12 months (southern regions) are commonly water-limited based on a similar interpretation of the SPEI1-EVI correlation. Thus, woody vegetation in normal periods shifts from energy limitation when the GS is short to water limitation when it is long, while herbaceous vegetation is consistently controlled by hydrological conditions (Figure 3).

The sensitivity of EVI changes in short-GS regions when contrasting post-drought periods to normal periods. Herbaceous vegetation shows a pronounced increase in sensitivity to water availability (black '+' to red '+' with $\beta_{leg} > 0$) and more negative sensitivity to radiation in both first and second GS (black '−' to red '−' with $\beta_{leg} < 0$). In contrast, woody vegetation shows relatively smaller changes in sensitivity to climate from the normal to post-drought periods (Figures 3a and 3b). Therefore, the normally water-limited herbaceous ecosystems become more water-limited (i.e., unchanged signs for SPEI1 and soil moisture in Figures 3a and 3b), while the normally energy-limited woody vegetation tends to become water-limited (flipping from black '−' to red '+' for soil moisture during first and second GS and the opposite for temperature during first GS in Figures 3a and 3b).

For the long-GS regions (i.e., LOS of 5–12 months, panels, etc.), woody and herbaceous vegetation change their sensitivity to climatic conditions in a similar way during the first GS, but the changes for herbaceous vegetation are weaker compared with those in the short-GS regions (Figures 3a, 3c and 3e). Changes during the second GS of the long-GS regions are relatively small and less consistent compared with others (Figures 3d and 3f vs. Figure 3a–c,e). In addition, the arid ecosystems in general respond more positively to soil moisture increases,

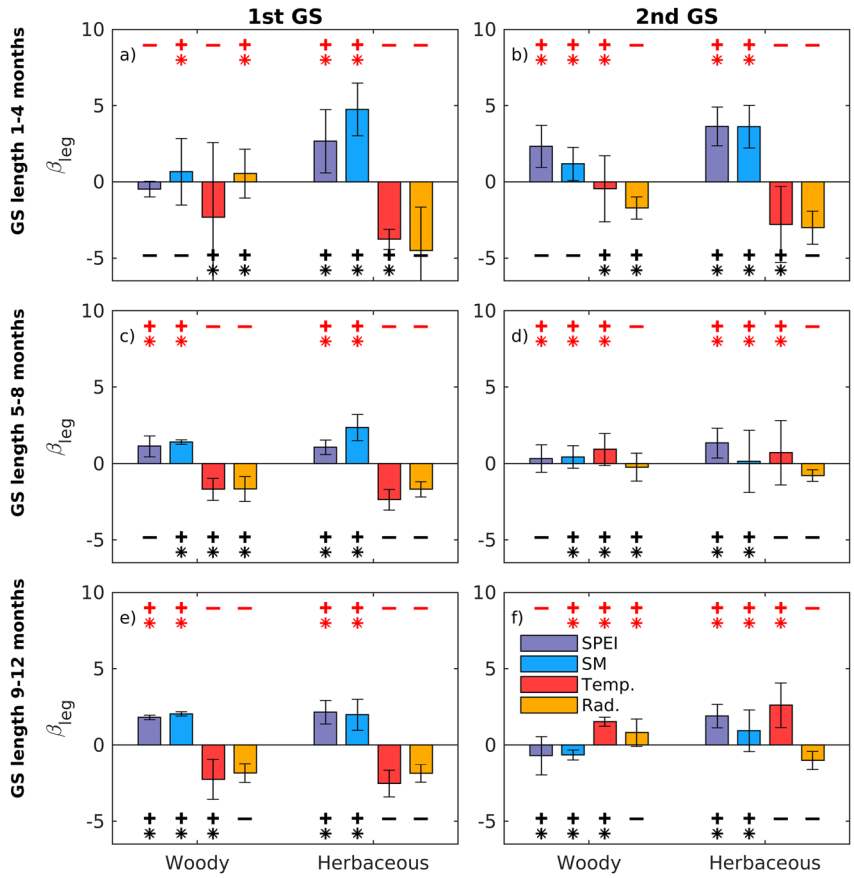

Figure 3. Legacy effects on the sensitivity of vegetation (β_{leg}) to growing conditions (Standardized Precipitation-Evapotranspiration Index for a time scale of 1 month, soil moisture, temperature, and radiation). Results are separated in panels according to growing-season length and post-drought growing seasons (i.e., first and second GS) as in Figure 2. Signs of '+' and '−' in black indicate the signs of β_{NM} (sensitivity of enhanced vegetation index to growing conditions during normal months); the corresponding signs in red are for β_{PD} (sensitivity during the post-drought months). Asterisks under the signs indicate values significantly different from zero ($p < 0.05$). Changes in β_{leg} for each ecosystem, including significance tests, can be found in Figures S5-S9 in Supporting Information S1. Error bars indicate the maximum and minimum of β_{leg} in different post-drought months at the level of land cover class. The definitions for the woody and the herbaceous vegetation, and the data screening approach are as in Figure 2.

compared with the humid ecosystems, with a larger distinction during the first GS (Figure S16 in Supporting Information S1).

4. Discussion and Conclusion

We quantified vegetation response to severe droughts as changes in vegetation greenness (Section 3.2) and its sensitivity to climate conditions (Section 3.3) during post-drought periods, using a novel location-specific definition of growing season based on MODIS EVI. We found that droughts negatively affect a large part of the vegetated land surface over the Northern Hemisphere with the strongest impacts on vegetation in arid regions (~20% loss of greenness on average, Figure S15 in Supporting Information S1). The greenness losses under severe droughts are partially compensated by significant greening from woody (~+5%, first GS) and herbaceous vegetation (~+5%, second GS), approximately 2–6 growing-season months after the droughts. Importantly, the drought legacy effects are also represented as ubiquitous changes in vegetation sensitivities to growing conditions, in which a prominent increase in sensitivity to soil moisture for herbaceous vegetation is found over the cold regions. To our knowledge, these findings based on large-scale vegetation activities have not been previously reported, and complement previous drought-impact studies. For example, the spatial pattern of drought-affected areas we found is in line with previous large-scale studies based on different physiological proxies (e.g., Orth et al., 2020;

X. Wu et al., 2018). The large-scale drought-induced greenness losses (5%–20% in Figure 2 and Figure S15 in Supporting Information S1) are also comparable with field studies (e.g., 20% in Dobbertin et al. [2010] and 19% in Limousin et al. [2012]).

Recovery is faster in woody deciduous than in woody evergreen vegetation over the mid-latitudes, as exemplified by the steeper slope of the recovery trajectories (Figure 2c). These differences in recovery might be due to the more adaptable leaf phenology of deciduous trees, or the insensitivity of EVI to leaf area changes for evergreen forests (Brando et al., 2010). For the former case, deciduous trees can reduce their leaf area thus partly avoiding droughts, and then grow new leaves when conditions improve (Manzoni et al., 2015; Schwartz, 2003; Vico et al., 2017) and prioritize the use of the reserve carbon for leaf regrowth (Poorter et al., 2012). The differences between woody deciduous and woody evergreen vegetation increase when using SPEI3 (Figure S10c in Supporting Information S1) while this is not the case for the shorter or longer drought time scales (SPEI1 or SPEI6). These disproportional changes in the inter-ecosystem difference in phenology recovery against drought duration are reminiscent of the drought-growth relationship derived from tree-ring analyses (D'Orangeville et al., 2018) in which differences in drought sensitivity across species are larger for 3-month drought than 1-month or 6-month droughts.

Vegetation sensitivities to SPEI and soil moisture (for all the chosen SPEI time scales) increase for almost all land cover classes and periods, and are particularly strong for the short-GS length herbaceous vegetation (e.g., Figures 3a, 3b and Figures S11a, S11b, S11g, S11h in Supporting Information S1). Such changes could result from plant-soil interactions, possibly associated with nutrient availability. If soil nutrient availability increases after droughts, increases in photosynthesis and growth are expected (Evans, 1989; de Vries et al., 2016), and could be amplified by the preferential biomass allocation to leaves (Gessler et al., 2017) potentially amplifying the phenological response to soil moisture. Indeed, rainfall manipulation experiments in semi-arid ecosystems identified a similar mechanism (e.g., Volder et al., 2010), presenting a greater increase in leaf-level net photosynthesis for C4 grasses than for the woody species after re-wetting. It is noteworthy that when severe droughts occur during LGS, the post-drought sensitivity changes become much weaker (Figure 3 vs. Figure S13 in Supporting Information S1) compared with those during EGS even though losses in EVI are similar (Figure 2 vs. Figure S12 in Supporting Information S1). A similar disproportional impact of the timing of drought occurrence is also seen in the field-measured changes in leaf photosynthesis for the first two GS (Misson et al., 2010), and in radial growth but with a later emergence than the changes in leaf photosynthesis after droughts (Bose et al., 2021).

While the greenness losses depend on the choice of SPEI (Figure S10 in Supporting Information S1), changes in vegetation sensitivity were unaffected (Figure S11 in Supporting Information S1). The time scale here reflects the period of cumulative water balance determining the types of droughts for analysis (Vicente-Serrano et al., 2010). For example, a short time-scale SPEI usually reflects drought intensity and could capture intermittent pulses of droughts, while a long time-scale SPEI reflects drought duration and could capture consecutive droughts. The larger greenness losses when using SPEI3 and SPEI6 (Figure S10 in Supporting Information S1) seem reasonable since the vegetation response intensifies linearly with drought duration (Orth et al., 2020).

Our analysis is based on 0.5-° spatial resolution and monthly EVI data. These scales are appropriate to assess large-scale changes but may mispresent local drought impacts where vegetation phenology is controlled by landscape heterogeneities (Zhang et al., 2017). Also, sub-grid interspecific differences in physiological sensitivity to droughts, and land-use variety, for example, with or without irrigation (Bodner et al., 2015), may affect our interpretation. Higher resolution and higher temporal frequency data could help improve local-scale and more subtle sub-seasonal impacts. In addition, employing multiple physiological proxies, including phenological products based on solar-induced chlorophyll fluorescence or passive microwave vegetation optical depth reflecting structural changes in vegetation (Guan et al., 2017; Meroni et al., 2009), may help reduce result uncertainty and may provide mechanistic insights on vegetation responses.

To conclude, our study leverages a location-specific definition of the growing season (Wu, Vico, et al., 2021), to detect large-scale vegetation phenological changes under changing climate. With this approach, we find prominent sub-seasonal drought legacy effects over the Northern Hemisphere, mainly represented as significant vegetation greening and increases in the sensitivity of herbaceous vegetation to hydrological conditions in different post-drought months during the first two post-drought growing seasons. The legacy effects on sensitivity tend

to be larger on herbaceous vegetation compared with woody vegetation, regardless of the chosen drought time scales.

Data Availability Statement

MODIS EVI composite data products (Didan et al., 2015) can be downloaded from the Land Processes Distributed Active Archive Centre (LP DAAC) (https://doi.org/10.5067/MODIS/MOD13C1.006). The MODIS land cover dataset MCD12C1 (Friedl et al., 2002) is available from https://doi.org/10.5067/MODIS/MCD12C1.006. ERA5 reanalysis data (Hersbach et al., 2020) is available from https://doi.org/10.24381/cds.f17050d7. CRU TS404 (Harris et al., 2020) is available from https://crudata.uea.ac.uk/cru/data/hrg/cru_ts_4.04/. The Global Land Evaporation Amsterdam Model (GLEAM) output (Martens et al., 2017) is available from https://www.gleam.eu/. The SPEI datasets v2.6 (Vicente-Serrano et al., 2010) at different time scales (up to December 2018) are available from https://spei.csic.es/database.html. The Global Aridity Index can be downloaded from the CGIAR Consortium for Spatial Information (CGIAR-CSI, https://cgiarcsi.community/data/global-aridity-and-pet-database/). The ESA CCI Land Cover time-series v2.0.7 (ESA, 2017) is downloaded from http://maps.elie.ucl.ac.be/CCI/viewer/download.php.

Acknowledgments
This research was supported by the Swedish Research Council for Sustainable Development (FORMAS) under Grant 2018-00968. GV was also partially supported by the European Commission and the Swedish Research Council FORMAS (Grant No. 2018-02787) in the frame of the collaborative international consortium iAqueduct financed under the 2018 Joint call of the WaterWorks 2017 ERA-NET Cofund. MW was also partially supported by the Swedish National Space Agency, SNSA (Dnr 2021-00111).

References

Adams, H. D., Guardiola-Claramonte, M., Barron-Gafford, G. A., Villegas, J. C., Breshears, D. D., Zou, C. B., et al. (2009). Temperature sensitivity of drought-induced tree mortality portends increased regional die-off under global-change-type drought. *Proceedings of the National Academy of Sciences of the United States of America*, *106*(17), 7063–7066. https://doi.org/10.1073/pnas.0901438106

Allen, C. D., Breshears, D. D., & McDowell, N. G. (2015). On underestimation of global vulnerability to tree mortality and forest die-off from hotter drought in the Anthropocene. *Ecosphere*, *6*(8), art129. https://doi.org/10.1890/es15-00203.1

Allen, C. D., Macalady, A. K., Chenchouni, H., Bachelet, D., McDowell, N., Vennetier, M., et al. (2010). A global overview of drought and heat-induced tree mortality reveals emerging climate change risks for forests. *Forest Ecology and Management*, *259*(4), 660–684. https://doi.org/10.1016/j.foreco.2009.09.001

Anderegg, L. D. L., Anderegg, W. R. L., & Berry, J. A. (2013). Not all droughts are created equal: Translating meteorological drought into woody plant mortality. *Tree Physiology*, *33*(7), 701–712. https://doi.org/10.1093/treephys/tpt044

Anderegg, W. R. L., Schwalm, C., Biondi, F., Camarero, J. J., Koch, G., Litvak, M., et al. (2015). Pervasive drought legacies in forest ecosystems and their implications for carbon cycle models. *Science*, *349*(6247), 528–532. https://doi.org/10.1126/science.aab1833

Bastos, A., Orth, R., Reichstein, M., Ciais, P., Viovy, N., Zaehle, S., et al. (2021a). Vulnerability of European ecosystems to two compound dry and hot summers in 2018 and 2019. *Earth System Dynamics*, *12*(4), 1015–1035. https://doi.org/10.5194/esd-12-1015-2021

Bastos, A., Orth, R., Reichstein, M., Ciais, P., Viovy, N., Zaehle, S., et al. (2021b). Increased vulnerability of European ecosystems to two compound dry and hot summers in 2018 and 2019. *Earth System Dynamics*. https://doi.org/10.5194/esd-2021-19

Blackman, C. J., Brodribb, T. J., & Jordan, G. J. (2009). Leaf hydraulics and drought stress: Response, recovery and survivorship in four woody temperate plant species. *Plant, Cell and Environment*, *32*(11), 1584–1595. https://doi.org/10.1111/j.1365-3040.2009.02023.x

Bodner, G., Nakhforoosh, A., & Kaul, H.-P. (2015). Management of crop water under drought: A review. *Agronomy for Sustainable Development*, *35*(2), 401–442. https://doi.org/10.1007/s13593-015-0283-4

Bose, A. K., Scherrer, D., Camarero, J. J., Ziche, D., Babst, F., Bigler, C., et al. (2021). Climate sensitivity and drought seasonality determine post-drought growth recovery of Quercus petraea and Quercus robur in Europe. *The Science of the Total Environment*, *784*, 147222. https://doi.org/10.1016/j.scitotenv.2021.147222

Brando, P. M., Goetz, S. J., Baccini, A., Nepstad, D. C., Beck, P. S. A., & Christman, M. C. (2010). Seasonal and interannual variability of climate and vegetation indices across the Amazon. *Proceedings of the National Academy of Sciences*, *107*(33), 14685–14690. https://doi.org/10.1073/pnas.0908741107

Bréda, N., Huc, R., Granier, A., & Dreyer, E. (2006). Temperate forest trees and stands under severe drought: A review of ecophysiological responses, adaptation processes and long-term consequences. *Annals of Forest Science*, *63*(6), 625–644.

Brodribb, T. J., Bowman, D. J. M. S., Nichols, S., Delzon, S., & Burlett, R. (2010). Xylem function and growth rate interact to determine recovery rates after exposure to extreme water deficit. *New Phytologist*, *188*(2), 533–542. https://doi.org/10.1111/j.1469-8137.2010.03393.x

Brun, P., Psomas, A., Ginzler, C., Thuiller, W., Zappa, M., & Zimmermann, N. E. (2020). Large-scale early-wilting response of Central European forests to the 2018 extreme drought. *Global Change Biology*, *26*(12), 7021–7035. https://doi.org/10.1111/gcb.15360

Cailleret, M., Jansen, S., Robert, E. M. R., Desoto, L., Aakala, T., Antos, J. A., et al. (2017). A synthesis of radial growth patterns preceding tree mortality. *Global Change Biology*, *23*(4), 1675–1690. https://doi.org/10.1111/gcb.13535

Clark, J. S., Iverson, L., Woodall, C. W., Allen, C. D., Bell, D. M., Bragg, D. C., et al. (2016). The impacts of increasing drought on forest dynamics, structure, and biodiversity in the United States. *Global Change Biology*, *22*(7), 2329–2352. https://doi.org/10.1111/gcb.13160

D'Orangeville, L., Maxwell, J., Kneeshaw, D., Pederson, N., Duchesne, L., Logan, T., et al. (2018). Drought timing and local climate determine the sensitivity of eastern temperate forests to drought. *Global Change Biology*, *24*(6), 2339–2351.

de Vries, F. T., Brown, C., & Stevens, C. J. (2016). Grassland species root response to drought: Consequences for soil carbon and nitrogen availability. *Plant and Soil*, *409*(1), 297–312. https://doi.org/10.1007/s11104-016-2964-4

Didan, K. (2015). MOD13C1 MODIS/Terra Vegetation Indices 16-Day L3 Global 0.05Deg CMG V006 [Dataset]. NASA EOSDIS Land Processes DAAC.

Diffenbaugh, N. S., Swain, D. L., & Touma, D. (2015). Anthropogenic warming has increased drought risk in California. *Proceedings of the National Academy of Sciences of the United States of America*, *112*(13), 3931–3936. https://doi.org/10.1073/pnas.1422385112

Dobbertin, M., Eilmann, B., Bleuler, P., Giuggiola, A., Graf Pannatier, E., Landolt, W., et al. (2010). Effect of irrigation on needle morphology, shoot and stem growth in a drought-exposed Pinus sylvestris forest. *Tree Physiology*, *30*(3), 346–360. https://doi.org/10.1093/treephys/tpp123

Dumouchel, W., & O'Brien, F. (1992). Integrating a robust option into a multiple regression computing environment. In *Computing and graphics in statistics* (pp. 41–48). Springer-Verlag.

ESA. Land Cover CCI Product User Guide Version 2. (2017). (Technical Report) Retrieved from maps.elie.ucl.ac.be/CCI/viewer/download/ESACCI-LC-Ph2-PUGv2_2.0.pdf

Evans, J. R. (1989). Photosynthesis and nitrogen relationships in leaves of C3 plants. *Oecologia*, *78*(1), 9–19. https://doi.org/10.1007/bf00377192

Fauset, S., Baker, T. R., Lewis, S. L., Feldpausch, T. R., Affum-Baffoe, K., Foli, E. G., et al. (2012). Drought-induced shifts in the floristic and functional composition of tropical forests in Ghana. *Ecology Letters*, *15*(10), 1120–1129. https://doi.org/10.1111/j.1461-0248.2012.01834.x

Friedl, M. A., McIver, D. K., Hodges, J. C. F., Zhang, X. Y., Muchoney, D., Strahler, A. H., et al. (2002). Global land cover mapping from MODIS: Algorithms and early results. *Remote Sensing of Environment*, *83*(1–2), 287–302. https://doi.org/10.1016/s0034-4257(02)00078-0

Gallé, A., & Feller, U. (2007). Changes of photosynthetic traits in beech saplings (Fagus sylvatica) under severe drought stress and during recovery. *Physiologia Plantarum*, *131*(3), 412–421.

Gazol, A., Camarero, J. J., Vicente-Serrano, S. M., Sánchez-Salguero, R., Gutiérrez, E., de Luis, M., et al. (2018). Forest resilience to drought varies across biomes. *Global Change Biology*, *24*(5), 2143–2158. https://doi.org/10.1111/gcb.14082

Gessler, A., Schaub, M., & McDowell, N. G. (2017). The role of nutrients in drought-induced tree mortality and recovery. *New Phytologist*, *214*(2), 513–520. https://doi.org/10.1111/nph.14340

Guan, K., Wu, J., Kimball, J. S., Anderson, M. C., Frolking, S., Li, B., et al. (2017). The shared and unique values of optical, fluorescence, thermal and microwave satellite data for estimating large-scale crop yields. *Remote Sensing of Environment*, *199*, 333–349. https://doi.org/10.1016/j.rse.2017.06.043

Harris, I., Osborn, T. J., Jones, P., & Lister, D. (2020). Version 4 of the CRU TS monthly high-resolution gridded multivariate climate dataset. *Scientific Data*, *7*(1), 109. https://doi.org/10.1038/s41597-020-0453-3

Hartmann, H., & Trumbore, S. (2016). Understanding the roles of nonstructural carbohydrates in forest trees - From what we can measure to what we want to know. *New Phytologist*, *211*(2), 386–403. https://doi.org/10.1111/nph.13955

Hersbach, H., Bell, B., Berrisford, P., Hirahara, S., Horányi, A., Muñoz-Sabater, J., et al. (2020). The ERA5 global reanalysis. *Quarterly Journal of the Royal Meteorological Society*, *146*(730), 1999–2049. https://doi.org/10.1002/qj.3803

Huschke, R. E. (1959). *Glossary of meteorology*. American Meteorological Society.

Iturbe-Ormaetxe, I., Escuredo, P. R., Arrese-Igor, C., & Becana, M. (1998). Oxidative damage in pea plants exposed to water deficit or paraquat. *Plant Physiology*, *116*(1), 173–181. https://doi.org/10.1104/pp.116.1.173

Jiao, W., Wang, L., & McCabe, M. F. (2021). Multi-sensor remote sensing for drought characterization: Current status, opportunities and a roadmap for the future. *Remote Sensing of Environment*, *256*, 112313. https://doi.org/10.1016/j.rse.2021.112313

Kannenberg, S. A., Novick, K. A., Alexander, M. R., Maxwell, J. T., Moore, D. J. P., Phillips, R. P., & Anderegg, W. R. L. (2019). Linking drought legacy effects across scales: From leaves to tree rings to ecosystems. *Global Change Biology*, *25*(9), 2978–2992. https://doi.org/10.1111/gcb.14710

Konings, A. G., Rao, K., & Steele-Dunne, S. C. (2019). Macro to micro: Microwave remote sensing of plant water content for physiology and ecology. *New Phytologist*, *223*(3), 1166–1172. https://doi.org/10.1111/nph.15808

Limousin, J.-M., Rambal, S., Ourcival, J.-M., Rodríguez-Calcerrada, J., Pérez-Ramos, I. M., Rodríguez-Cortina, R., et al. (2012). Morphological and phenological shoot plasticity in a Mediterranean evergreen oak facing long-term increased drought. *Oecologia*, *169*(2), 565–577. https://doi.org/10.1007/s00442-011-2221-8

Manzoni, S., Vico, G., Thompson, S., Beyer, F., & Weih, M. (2015). Contrasting leaf phenological strategies optimize carbon gain under droughts of different duration. *Advances in Water Resources*, *84*, 37–51. https://doi.org/10.1016/j.advwatres.2015.08.001

Martens, B., Miralles, D., Lievens, H., van der Schalie, R., de Jeu, R. A. M., Fernández-Prieto, D., et al. (2017). GLEAM v3: Satellite-based land evaporation and root-zone soil moisture. *Geoscientific Model Development*, *10*(5), 1903–1925. https://doi.org/10.5194/gmd-10-1903-2017

McDowell, N. G., Coops, N. C., Beck, P. S. A., Chambers, J. Q., Gangodagamage, C., Hicke, J. A., et al. (2015). Global satellite monitoring of climate-induced vegetation disturbances. *Trends in Plant Science*, *20*(2), 114–123. https://doi.org/10.1016/j.tplants.2014.10.008

Mencuccini, M., Minunno, F., Salmon, Y., Martínez-Vilalta, J., & Hölttä, T. (2015). Coordination of physiological traits involved in drought-induced mortality of woody plants. *New Phytologist*, *208*(2), 396–409. https://doi.org/10.1111/nph.13461

Meroni, M., Rossini, M., Guanter, L., Alonso, L., Rascher, U., Colombo, R., & Moreno, J. (2009). Remote sensing of solar-induced chlorophyll fluorescence: Review of methods and applications. *Remote Sensing of Environment*, *113*(10), 2037–2051. https://doi.org/10.1016/j.rse.2009.05.003

Misson, L., Limousin, J.-M., Rodriguez, R., & Letts, M. G. (2010). Leaf physiological responses to extreme droughts in Mediterranean Quercus ilex forest. *Plant, Cell and Environment*, *33*(11), 1898–1910. https://doi.org/10.1111/j.1365-3040.2010.02193.x

Orth, R., Destouni, G., Jung, M., & Reichstein, M. (2020). Large-scale biospheric drought response intensifies linearly with drought duration in arid regions. *Biogeosciences*, *17*(9), 2647–2656. https://doi.org/10.5194/bg-17-2647-2020

Pastorello, G., Trotta, C., Canfora, E., Chu, H., Christianson, D., Cheah, Y.-W., et al. (2020). The FLUXNET2015 dataset and the ONEFlux processing pipeline for eddy covariance data. *Scientific Data*, *7*(1), 225.

Poorter, H., Niklas, K. J., Reich, P. B., Oleksyn, J., Poot, P., & Mommer, L. (2012). Biomass allocation to leaves, stems and roots: Meta-analyses of interspecific variation and environmental control. *New Phytologist*, *193*(1), 30–50. https://doi.org/10.1111/j.1469-8137.2011.03952.x

Posch, S., & Bennett, L. T. (2009). Photosynthesis, photochemistry and antioxidative defence in response to two drought severities and with re-watering in Allocasuarina luehmannii. *Plant Biology*, *11*(Suppl 1), 83–93. https://doi.org/10.1111/j.1438-8677.2009.00245.x

Prudhomme, C., Giuntoli, I., Robinson, E. L., Clark, D. B., Arnell, N. W., Dankers, R., et al. (2014). Hydrological droughts in the 21st century, hotspots and uncertainties from a global multimodel ensemble experiment. *Proceedings of the National Academy of Sciences of the United States of America*, *111*(9), 3262–3267. https://doi.org/10.1073/pnas.1222473110

Reichstein, M., Bahn, M., Ciais, P., Frank, D., Mahecha, M. D., Seneviratne, S. I., et al. (2013). Climate extremes and the carbon cycle. *Nature*, *500*(7462), 287–295. https://doi.org/10.1038/nature12350

Resco, V., Ewers, B. E., Sun, W., Huxman, T. E., Weltzin, J. F., & Williams, D. G. (2009). Drought-induced hydraulic limitations constrain leaf gas exchange recovery after precipitation pulses in the C3 woody legume, Prosopis velutina. *New Phytologist*, *181*(3), 672–682. https://doi.org/10.1111/j.1469-8137.2008.02687.x

Ruehr, N. K., Grote, R., Mayr, S., & Arneth, A. (2019). Beyond the extreme: Recovery of carbon and water relations in woody plants following heat and drought stress. *Tree Physiology*, *39*(8), 1285–1299. https://doi.org/10.1093/treephys/tpz032

Scherrer, D., Bader, M. K.-F., & Körner, C. (2011). Drought-sensitivity ranking of deciduous tree species based on thermal imaging of forest canopies. *Agricultural and Forest Meteorology*, *151*(12), 1632–1640. https://doi.org/10.1016/j.agrformet.2011.06.019

Schwartz, M. D. (2003). *Phenology: An Integrative Environmental Science*. Springer.

Seneviratne, S., Nicholls, N., Easterling, D., Goodess, C., Kanae, S., Kossin, J., et al. (2012). *Changes in climate extremes and their impacts on the natural physical environment*. Columbia University. https://doi.org/10.7916/D8-6NBT-S431

Steele, C. L., Lewinsohn, E., & Croteau, R. (1995). Induced oleoresin biosynthesis in grand fir as a defense against bark beetles. *Proceedings of the National Academy of Sciences of the United States of America*, *92*(10), 4164–4168. https://doi.org/10.1073/pnas.92.10.4164

Trugman, A. T., Detto, M., Bartlett, M. K., Medvigy, D., Anderegg, W. R. L., Schwalm, C., et al. (2018). Tree carbon allocation explains forest drought-kill and recovery patterns. *Ecology Letters*, *21*(10), 1552–1560. https://doi.org/10.1111/ele.13136

van der Molen, M. K., Dolman, A. J., Ciais, P., Eglin, T., Gobron, N., Law, B. E., et al. (2011). Drought and ecosystem carbon cycling. *Agricultural and Forest Meteorology*, *151*(7), 765–773.

Vicente-Serrano, S. M., Beguería, S., & López-Moreno, J. I. (2010). A multiscalar drought index sensitive to global warming: The standardized precipitation evapotranspiration index. *Journal of Climate*, *23*(7), 1696–1718. https://doi.org/10.1175/2009jcli2909.1

Vicente-Serrano, S. M., McVicar, T. R., Miralles, D. G., Yang, Y., & Tomas-Burguera, M. (2020). Unraveling the influence of atmospheric evaporative demand on drought and its response to climate change. *Climate Change*, *11*(2), e632. https://doi.org/10.1002/wcc.632

Vico, G., Dralle, D., Feng, X., Thompson, S., & Manzoni, S. (2017). How competitive is drought deciduousness in tropical forests? A combined eco-hydrological and eco-evolutionary approach. *Environmental Research Letters*, *12*(6), 065006. https://doi.org/10.1088/1748-9326/aa6f1b

Volder, A., Tjoelker, M. G., & Briske, D. D. (2010). Contrasting physiological responsiveness of establishing trees and a C4 grass to rainfall events, intensified summer drought, and warming in oak savanna. *Global Change Biology*, *16*(12), 3349–3362. https://doi.org/10.1111/j.1365-2486.2009.02152.x

Wu, M., Smith, B., Schurgers, G., Ahlström, A., & Rummukainen, M. (2021). Vegetation-climate feedbacks enhance spatial heterogeneity of pan-amazonian ecosystem states under climate change. *Geophysical Research Letters*, *48*(8). https://doi.org/10.1029/2020gl092001

Wu, M., Vico, G., Manzoni, S., Cai, Z., Bassiouni, M., Tian, F., et al. (2021). Early growing season anomalies in vegetation activity determine the large-scale climate-vegetation coupling in Europe. *Journal of Geophysical Research: Biogeosciences*, *126*. https://doi.org/10.1029/2020jg006167

Wu, X., Liu, H., Li, X., Ciais, P., Babst, F., Guo, W., et al. (2018). Differentiating drought legacy effects on vegetation growth over the temperate Northern Hemisphere. *Global Change Biology*, *24*(1), 504–516. https://doi.org/10.1111/gcb.13920

Xu, C., McDowell, N. G., Fisher, R. A., Wei, L., Sevanto, S., Christoffersen, B. O., et al. (2019). Increasing impacts of extreme droughts on vegetation productivity under climate change. *Nature Climate Change*, *9*(12), 948–953. https://doi.org/10.1038/s41558-019-0630-6

Xu, Z., Zhou, G., & Shimizu, H. (2010). Plant responses to drought and rewatering. *Plant Signaling & Behavior*, *5*(6), 649–654. https://doi.org/10.4161/psb.5.6.11398

Zhang, X., Wang, J., Gao, F., Liu, Y., Schaaf, C., Friedl, M., et al. (2017). Exploration of scaling effects on coarse resolution land surface phenology. *Remote Sensing of Environment*, *190*, 318–330. https://doi.org/10.1016/j.rse.2017.01.001

Zolina, O., Simmer, C., Belyaev, K., Gulev, S. K., & Koltermann, P. (2013). Changes in the duration of European wet and dry spells during the last 60 years. *Journal of Climate*, *26*(6), 2022–2047. https://doi.org/10.1175/jcli-d-11-00498.1